ACS APPLIED MATERIALS & INTERFACES

Research Article

www.acsami.org

# Surface and Structure Characteristics, Self-Assembling, and Solvent Compatibility of Holocellulose Nanofibrils

Jin Gu and You-Lo Hsieh*

Fiber and Poglymer Science, University of California, Davis, California 95616, United States

Supporting Information

**ABSTRACT:** Rice straw holocellulose was TEMPO-oxidized and mechanically defibrillated to produce holocellulose nanofibrils (HCNFs) at 33.7% yield (based on original rice straw mass), 4.6% higher yield than cellulose nanofibril (CNF) generated by the same process from pure rice straw cellulose. HCNFs were similar in lateral dimensions (2.92 nm wide, 1.36 nm thick) as CNF, but longer, less surface oxidized (69 vs 85%), and negatively charged (0.80 vs 1.23 mmol/g). HCNFs also showed higher affinity to hydrophobic surfaces than CNFs while still attracted to hydrophilic surfaces. By omitting hemicellulose/silica dissolution step, the two-step 2:1 toluene/ethanol extraction and acidified $NaClO_2$ (1.4%, pH 3−4, 70 °C, 6 h) delignification process for holocellulose was more streamlined than that of pure cellulose, while the resulting amphiphilic HCNFs were more hydrophobic and self-assembled into much finer nanofibers, presenting unique characteristics for new potential applications.

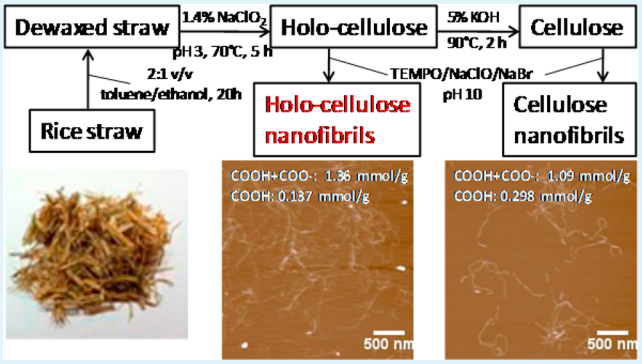


**KEYWORDS:** *holocellulose nanofibril, TEMPO oxidation, self-assembly, redispersion, hydrophobicity, rice straw*

## 1. INTRODUCTION

Nanocellulose is now considered as one of the most promising renewable reinforcement nanomaterials due to their biodegradability, outstanding mechanical properties, and light weight.[1] Commonly, nanocellulose is categorized into cellulose nanocrystals (CNCs) produced by removing noncrystalline domains with strong acid hydrolysis or cellulose nanofibrils (CNFs) defibrillated by high mechanical shear forces, all from pure cellulose. While both have nanoscale lateral dimensions, CNCs are rod-like, and CNFs are generally longer and more flexible.[2] By the nature of hydrolysis, CNC yields are typically less than 30%, depending on sources and processes, whereas CNFs are produced at much higher yields up to 100%.[3]

CNFs can be generated from various mechanically defibrillation methods of blending, grinding, high-pressure homogenization, and sometimes in combination; however, these methods consume significant energy (700−1400 MJ/kg), a limiting factor for large-scale production.[3] Pretreatment with enzyme hydrolysis or chemical oxidation has therefore been applied to reduce the energy input of mechanical defibrillation.[4−6] Among them, 2,2,6,6-tetramethylpyperidine-1-oxyl (TEMPO)-mediated oxidation of C6 primary hydroxyls to carboxyls is most reported.[7]

Increasing attention has been drawn to nanocellulose from sources other than pulp- or wood-derived cellulose. Rice is the third most produced cereal crop in the world, behind wheat and corn, but generates the most rice straw byproduct due to the higher crop residue to grain ratio, ca. 1−1.5 to 1.[8] Rice straw contains nearly 40% cellulose, close to wood,[9,10] which has been sulfuric acid hydrolyzed into CNCs,[9,11,12] mechanically defibrillated,[11] and TEMPO-oxidized and mechanically defibrillated into CNFs.[11] While the CNC from acid hydrolysis yielded only 6.4%, TEMPO-oxidation coupled with mechanical blending could optimize the CNF yield to a far superior 96.8%,[13] near full conversion. In these cases, pure cellulose was isolated from rice straw by an efficient three-step process to remove waxes, lignin, and hemicellulose in a sequential manner. In our attempt to further streamline the process, questions arose as to whether more nanocellulose may be derived from less purified cellulose such as holocellulose, that is, without removing hemicellulose, and how such nanocellulose is different from that derived from pure cellulose.

In pulping, the presence of hemicelluloses has shown to disrupt interfibrillar hydrogen bonding, inhibit the coalescent of cellulose microfibrils,[14] maintain the swelling capacity of the dried pulp,[15,16] and facilitate the defibrillation.[14,17] The presence of hemicellulose and lignin has shown to lengthen the reaction times for TEMPO oxidation of thermomechanical pulp,[18] while residual hemicelluloses in CNFs lowered the transmittance of CNF films.[3,7] Most recently, TEMPO-oxidized cellulose nanofibrils have been prepared from several plant holocelluloses[19,20] to show dissolution of most of hemicelluloses under the basic condition (pH 10), leaving ∼1−5% hemicellulose in the resulting nanofibrils, depending on the

Received: December 2, 2014
Accepted: January 30, 2015
Published: January 30, 2015





DOI: 10.1021/am5079489
ACS Appl. Mater. Interfaces 2015, 7, 4192−4201

plant sources.[20] However, how hemicelluloses affect the defibrillation of holocellulose or the behaviors of the resulting nanocellulose has not been clearly delineated.

This study was thus aimed to address these questions by deriving and characterizing nanofibrils from rice straw holocellulose and compare the holocellulose nanofibrils (HCNFs) with CNFs from pure rice straw cellulose. Holocellulose was isolated by dewaxed and delignified rice straw, then TEMPO oxidized using 5 and 10 mmol primary oxidant NaClO per gram of holocellulose followed by mechanical blending at varied lengths of time similar to the conditions previously reported for deriving CNFs from pure rice straw cellulose.[13] The defibrillation of rice straw holocellulose into nanofibrils and their yields, qualities (surface charge, morphologies, etc.) and self-assembling behaviors of HCNFs were characterized and compared to CNFs. Aqueous and organic dispersion and redispersion of self-assembled HCNFs and CNFs were studied extensively and correlated to their surface chemistry to further delineate the effects of residual hemicelluloses on the interfacial properties of nanofibrils.

## 2. MATERIALS AND METHODS

**2.1. Materials.** Rice straw (Calrose variety) was harvested in the Sacramento Valley in 2009, as reported previously.[12] Toluene (99.5%, ACS GR Fisher Scientific), ethanol (anhydrous, histological grade, Fisher Scientific), sodium chlorite ($NaClO_2$, 80%, Fluka), acetic acid glacial ($CH_3COOH$, 99.7%, ACS GR, EMD), potassium hydroxide (KOH, 85%, EM Science), hydrochloric acid (HCl, 1 N, Certified, Fisher Scientific), sodium hydroxide (NaOH, 1 N, Certified, Fisher Scientific), sodium hypochlorite (NaClO, 10.6%, reagent grade, Sigma−Aldrich), 2,2,6,6-tetramethylpyperidine-1-oxyl (TEMPO, 99.9%, Sigma-Aldrich), and sodium bromide (NaBr, BioXtra, 99.6%, Sigma−Aldrich) were used as received. Water used was purified by Milli-Q plus water purification system (Millipore Corporate, Billerica, MA).

**2.2. Removal of Wax, Lignin, and Hemicelluloses from Rice Straw.** Pure cellulose and holocellulose were prepared from rice straw. A three-step process was used to remove wax, lignin, and hemicelluloses in sequence from rice straw, as reported previously.[12] Briefly, milled rice straw powder (30 g) was first extracted with toluene/ethanol (2:1, v/v, 450 mL) mixture for 20 h to remove wax, pigments, and oils. The dewaxed rice straw was then transferred to 1.4% acidified $NaClO_2$ (1000 mL) at 70 °C for 5 h to dissolve lignin. The initial pH of the solution was adjusted to 3.0−4.0 by $CH_3COOH$. The delignified product was designated as holocellulose and used to prepare holocellulose nanofibrils. Pure cellulose was obtained by treating the holocellulose powder with 5% KOH at room temperature for 24 h and then at 90 °C for 2 h. During this process, the hemicelluloses and silica were dissolved in the alkali.

**2.3. Preparation of Cellulose Nanofibrils and Holocellulose Nanofibrils.** CNFs and HCNFs were prepared by TEMPO mediated oxidation followed by mechanical defibrillation using a previously reported procedure.[13] Briefly, 1 g of either pure cellulose or holocellulose, 0.016 g of TEMPO, and 0.1 g of NaBr were added to 100 mL of water. Oxidation reaction was initiated by adding either 5 mM or 10 mM NaClO and conducted at 9.8−10.2 pH (OAKTON pH/Con 510 series meter), adjusted by adding 0.5 M NaOH at room temperature. The oxidation reaction was considered complete when no further decrease in pH was observed. The TEMPO-oxidized cellulose or holocellulose suspension was pH adjusted to 7 with 0.5 M HCl, centrifuged at 5000 rpm for 15 min, dialyzed against water (Spectrum/Pro dialysis membrane, MWCO: 12000 Da) to remove salts and other small molecules and designated as C5, HC5, and HC10, where the number indicated NaClO concentration used. The C and HC suspensions of 0.2% (w/v) were mechanically blended at 37 000 rpm (Vitamix 5200) at varying lengths of times (15−60 min) and then centrifuged at 5000 rpm for 15 min to obtain supernatants, which were designated as CNF5-30, HCNF5-30, HCNF5-60, HCNF10-1,5 and HCNF10-30, where the second number denotes mechanical blending time in minutes. All yields were based on the mass of rice straw, and all the nanofibril concentrations mentioned below are based on weight percentage in unit volume of solvents.

**2.4. Characterization of CNFs, HCNFs, and Their Assembled Solids.** CNFs and HCNFs were characterized as aqueous suspensions, as in the case for $COOH/COO^-$ concentration by conductometric titration, or as air-dried samples from aqueous suspensions for their dimensions by transmission electron microscopy (TEM) and atomic force microscopy (AFM). Frozen (liquid nitrogen, −196 °C) and freeze-dried (−50 °C) solids were characterized by scanning electron microscopy (SEM), Fourier transform infrared spectroscopy (FTIR), thermogravimetric analysis (TGA), and X-ray diffraction (XRD).

TEM samples were prepared by depositing a 10 μL drop of 0.01% aqueous suspension of either CNF or HCNF onto carbon-coated TEM grids (300-mesh copper, Formvar-carbon, Ted Pella, Inc.). The excess liquid was removed by blotting with a filter paper after 10 min. Uranyl acetate solution (2%) was used to negatively stain the specimens. The excess staining solution was removed by blotting with a filter paper after 10 min. A Philips CM12 transmission electron microscope operated at a 100 kV accelerating voltage was used to obtain the morphology of the nanofibrils. The image was processed through ImageJ and the average width of the nanofibrils was determined from about 150 individual nanofibrils.

AFM samples were prepared by depositing 10 μL (0.0005 or 0.0001%) of each suspension onto freshly cleaved mica or highly ordered pyrolytic graphite (HOPG, grade ZYB, prod No.626-1, Ted Pella, Inc.) surfaces and air-dried. The samples were scanned with an atomic force microscope (Asylum-Research MFP-3D) under the ambient condition using tapping mode with OMCL-AC160TS standard silicon probes (cantilever spring constant 42 N/m). The scan rate was set to 1 Hz. The height images and profiles were processed with Igor Pro 6.21 software, and 150 height values were used to calculate the average thickness of either CNFs or HCNFs.

For the conductometric titration, the total COOH and $COO^-$ content of the nanofibrils was measured by first adding a certain amount of 1 N HCl to 50 mL of 0.1% suspension to protonate the carboxyl groups. After that, the suspension was titrated with 0.02 M NaOH solution. During the titration, the conductivity values of the suspension were recorded by an OAKTON pH/Con 510 series meter. The total COOH and $COO^-$ content ($\sigma_{COOH+COO-}$, in mmol per gram of nanofibril) was determined as follows:

$$\sigma_{COOH+COO-} = \frac{cv}{m} = \frac{c(v_1 - v_2)}{m} \quad (1)$$

where $c$ is the NaOH concentration (0.02 M), $m$ is the mass of the suspension (0.050 g), and $v_1$ and $v_2$ are NaOH volumes (in mL) used from neutralizing the added HCl and carboxylic acid groups, respectively. The amount of COOH groups in the nanofibrils ($\sigma_{COOH}$, in mmol per gram of nanofibril) was measured by adding 0.02 M NaOH solution directly to the suspension without first adding HCl and was determined as follows:

$$\sigma_{COOH} = \frac{cv_3}{m} \quad (2)$$

where $v_3$ is the volume of NaOH used to neutralize carboxylic acid groups.

FTIR specimens were prepared by mixing freeze-dried CNF or HCNF with KBr at 1:100, w/w CNF:KBr ratio. A Thermo Nicolet 6700 spectrometer was used to obtain the FTIR spectra from 64 scans over 4000−400 $cm^{-1}$ at a resolution of 4 $cm^{-1}$ under transmission mode.

SEM samples were prepared by freeze-drying two different concentrations (0.1% and 0.01%) of HCNF5-30, mounting with conductive carbon tape and sputter coating with gold. The SEM images were obtained by a field emission scanning electron microscope (FE-SEM) (XL 30-SFEG, FEI/Philips, USA) at a 5 mm working distance and 5 kV accelerating voltage. The average diameters of


DOI: 10.1021/am5079489
ACS Appl. Mater. Interfaces 2015, 7, 4192−4201

freeze-dried fibers were obtained from more than 100 individual fibers by an image software (ImageJ, NIH, USA).

XRD spectra of freeze-dried samples were obtained with a Scintag XDS 2000 powder diffractometer using a Ni filtered Cu−K$\alpha$ radiation generated at 45 kV and 40 mA. Diffractograms were collected at a rate of 2°/min from 5 to 40° 2$\theta$. The crystallinity index (CrI), crystallite dimensions and the primary C6 hydroxyl groups on cellulose crystal surfaces were determined following a previous study.[13] More details could be found in the Supporting Information.

A TGA-50 thermogravimetric analyzer (Shimadzu) was used to obtain the weight loss of freeze-dried CNF or HCNF with increasing temperature. Each sample (~5 mg) was heated from 26 to 500 °C at a rate of 10 °C/min under $N_2$ atmosphere (50 mL/min).

**2.5. Dispersion of CNF or HCNF in Organic Solvents.** CNFs and HCNFs were freeze-dried at 0.1% concentration and transferred to water, ethanol, acetone, dimethylformamide (DMF), and chloroform to form 0.1% suspensions. Three methods were used individually or in combination to redisperse the nanofibrils in the solvents. Mechanical stirring with a magnetic stir bar (1200 rpm) and low power ultrasonication (40 kHz, 130 w, Branson 2510) were used in combination. The mixtures were mechanically stirred for 10 min and then sonicated for another 10 min as one cycle, and the cycle was repeated 10 times for all mixtures. High-power ultrasonication (20 kHz, 600 w, MisonixSonicator S-4000) was applied alone for 2 min to all mixtures. The mixtures were settled for 1 day for images.

A solvent exchange process was also used to prepare organic solvent dispersions of CNF or HCNF, all at 0.1%. DMF was added to CNF5-30 or HCNF5-30 aqueous suspension (1:1 v/v). Water was evaporated at reduced pressure (50 °C, 40 min). The mixture was sonicated for 2 min using the high-power ultrasonic homogenizer as above. To prepare CNF dispersions in ethanol or acetone, a different solvent exchange process was used because the boiling point of ethanol or acetone is lower than that of water. Acetone or ethanol was gently added on top of the aqueous nanofibrils dispersion (2 mg/mL) at 3:1 organic solvent/water. A phase contained mainly organic solvent formed on the top of the aqueous dispersion and the top phase was exchanged with fresh solvent 1−2 times daily without disrupting the bottom phase. A mechanically coherent nanofibril gel formed at the bottom of the glass vial after 4−5 days. When solvent mixing was no longer visible (i.e., the refractive index gradients at the sol/gel interface disappeared), the organogel was released from the vial and washed with the organic solvent three times. The organogels were merged to the organic solvents and subjected to high-power ultrasonication to make 0.1% CNF/organic solvent mixtures.

## 3. RESULTS AND DISCUSSION

**3.1. Isolation of Holocellulose Nanofibrils (HCNFs).** Pure cellulose was isolated from cleaned and dried rice straw powder following the previously established three-step process described earlier.[9] Holocellulose was produced by omitting the third alkaline extraction step in lightly yellow color. The holocellulose and pure cellulose yields were 72.8 and 35.1%, respectively (Table 1), the latter close to previously reported values.[9,21] The mass of holocellulose was 37.7% higher than that of pure cellulose; the holocellulose is thought to contain hemicelluloses as well as silica, which is not soluble in either 2/1 toluene/ethanol or acidified $NaClO_2$. The light yellow color of holocellulose also indicates a trace amount of lignin. Assuming the reported 5−18% silica in rice straw[10,22,23] and negligible lignin, the hemicellulose content in the holocellulose would be as low as 20% to as high as 33%.

Both pure cellulose and holocellulose were TEMPO-oxidized using either 5 or 10 mM NaClO per gram of cellulose/holocellulose then mechanically defibrillated into CNFs and HCNFs, respectively (Table 1). Cellulose TEMPO oxidized with 5 mM NaClO produced 87% oxidized cellulose C5 (30.8% of rice straw), losing 13% to dissolution. The same TEMPO oxidation of holocellulose yielded 52% HC5 (37.9% of rice straw), or 48% holocellulose dissolved. The nearly 35% mass loss from TEMPO oxidation of holocellulose was expected from the oxidation of substantial hemicelluloses present in addition to amorphous cellulose. Therefore, most, if not all, hemicelluloses were removed, and some silica may have also dissolved under basic conditions. Following 30 min of mechanical blending, 88.9% of the oxidized holocellulose HC5 defibrillated to yield 33.7% HCNF5-30, higher than the 29.1% yield of CNF5-30 (94.5% of C5), both based on original rice straw. When the blended suspensions were centrifuged, no precipitate was observed from the CNF5-30 suspension, while a small amount of precipitate was observed from HCNF5-30, attributing residual fiber fragments and/or silica. This observation was also consistent with the lower defibrillated efficiency of HC5 (88.9%), as compared to C5 (94.5%). Doubling blending time to 60 min or NaClO to 10 mM lowered the yields by 4.9% and 4.0%, respectively. Therefore, the optimal condition to produce the most HCNFs was TEMPO oxidation with 5 mM NaClO followed by 30 min of mechanical blending for holocellulose, the same as for cellulose, but at 4.6% higher yield.

The FTIR spectra of rice straw holocellulose exhibited C=O stretching at 1729 $cm^{-1}$ that was consistent with the hemicellulose carboxyl as well as C−O stretching at 1245 $cm^{-1}$, indicating the presence of xylan, a major hemicellulose in rice straw (Figure 1).[14] Absence of these peaks from pure cellulose confirmed the removal of hemicelluloses. The C−O stretching peak (1245 $cm^{-1}$) was less intense in HCNF5-30,

**Table 1. Isolation and Defibrillation Product Yields (All Based on Original Rice Straw Mass)**

| rice straw products | yield (%) | TEMPO oxidation | yield (%) | blending | yield (%) |
|---|---|---|---|---|---|
| dewaxed rice straw | 94.4 | | | | |
| holocellulose | 72.8 | HC5 | 37.9 | HCNF5-30 | 33.7 |
| | | | | HCNF5-60 | 28.8 |
| | | HC10 | 34.8 | HCNF10-15 | 31.7 |
| | | | | HCNF10-30 | 29.7 |
| cellulose | 35.5 | C5 | 30.8 | CNF5-30 | 29.1 |

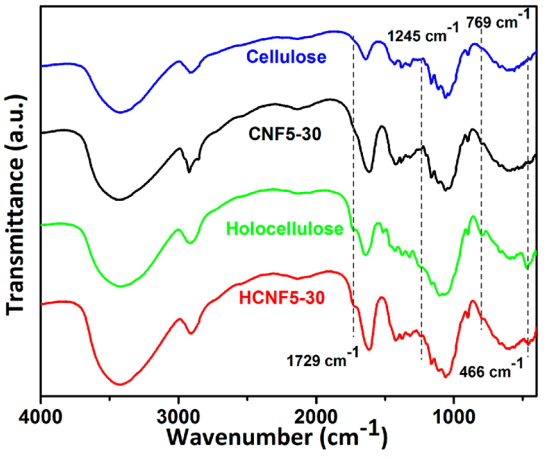


**Figure 1.** FTIR spectrum of cellulose, holocellulose, CNF5-30, and HCNF5-30.



DOI: 10.1021/am5079489
ACS Appl. Mater. Interfaces 2015, 7, 4192−4201

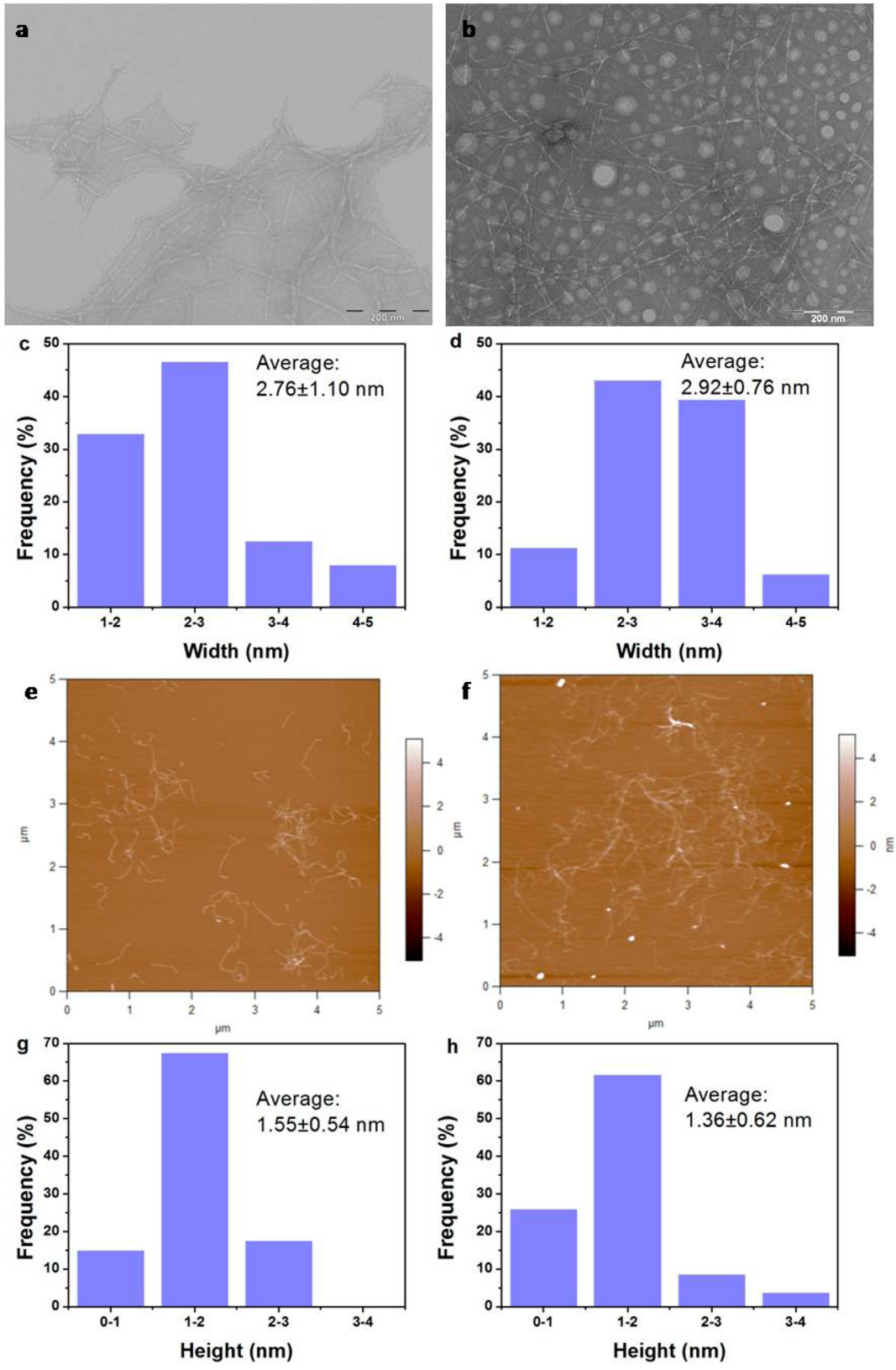


**Figure 2.** TEM images of (a) CNF-30 and (b) HCNF5-30; width distributions of (c) CNF5-30 and (d) HNCF5-30; TEM images of (e) CNF5-30 and (f) HCNF5-30; and height distributions of (g) CNF5-30 and (h) HCNF5-30. Width and height distributions were obtained via TEM and AFM, respectively.

consistent with reduced hemicellulose content and yield. The C═O stretching at 1729 $cm^{-1}$ was detected in both HCNF5-30 and CNF5-30, confirming C6 primary hydroxyl conversion to carboxyls from TEMPO oxidation of both cellulose and hemicelluloses. The bands at 796 and 466 $cm^{-1}$ detected in holocellulose were attributed to Si−O−Si stretching, confirm-



DOI: 10.1021/am5079489
ACS Appl. Mater. Interfaces 2015, 7, 4192−4201

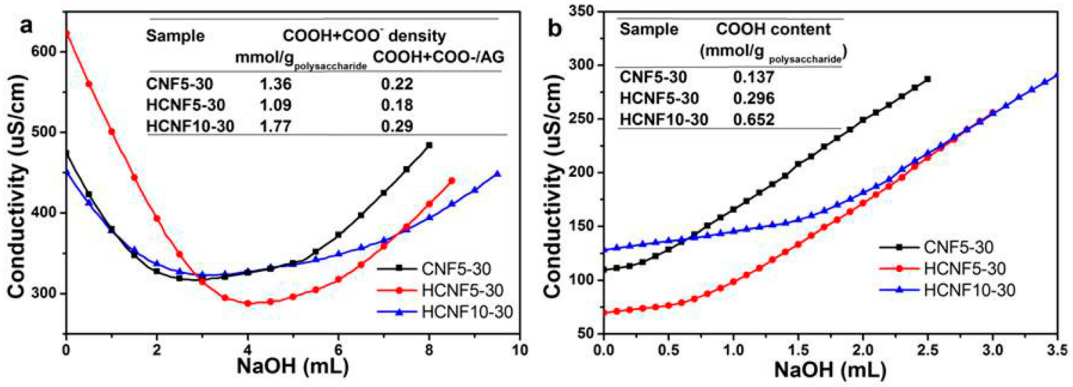


**Figure 3.** Conductometric titration curves (a) with HCl added and (b) without HCl added.

ing the presence of silica, the same as previously reported.[9] Less intensive Si−O−Si peaks were observed in HCNF5-30 than in holocellulose, indicating partial removal of silica that was observed as the precipitate after defibrillation and centrifugation. Neither silica peak was observed in pure cellulose and CNF5-30, confirming complete silica removal by the alkali, the third cellulose isolation step. The FTIR spectrum of a large fiber precipitate separated by centrifugation following mechanical defibrillation of HC5 showed intense Si−O−Si peaks (Figure S1, Supporting Information), clearly indicating the presence of silica and consistent with the expected precipitation of silica at neutral pH. Therefore, FTIR confirmed the presence of hemicelluloses and silica in holocellulose and their reduced extents in HCNFs. This is consistent with the small residual amount of xylan (~3%) and silica from similarly TEMPO-oxidized rice straw holocellulose.[20]

**3.2. Dimensions and Surface Carboxyl Content of HCNFs.** The length and width measured by TEM showed CNF5-30 to be 2.76 ± 1.10 nm wide and hundreds of nanometers to 2 μm long (Figure 2a). HCNF5-30 had an average width of 2.92 ± 1.10 nm (Figure 2b), similar to CNF5-30, but contained more 3−5 nm wide nanofibrils (Figure 2d). The AFM height images showed the average thicknesses of CNF5-30 and HCNF5-30 to be 1.55 ± 0.54 nm and 1.36 ± 0.62 nm, respectively, and again, similarly (Figure 2e−h). However, CNF5-30 contained some shorter 100−300 nm long nanofibrils (Figure 2a) while almost all HCNF5-30 nanofibrils exceeded 500 nm in length (Figure 2b). These data are consistent with previous studies with TEMPO-oxidized cellulose nanofibrils from various plant sources (i.e., the thickness of the nanofibrils is 1−2 nm, and the width is 3−5 nm).[20,24,25] Overall, according to our measurements, some HCNFs appear wider and longer than CNFs, but their average dimensions are not significantly different. The white spots shown in the AFM images of HCNF5-30 (Figure 2e) may be silica particles, as evidenced in the FTIR spectrum.

During TEMPO oxidation at pH 10, the newly formed C6 carboxyls (COOH) reacted with NaOH to form carboxylates ($COO^-$). Neutralization after the oxidation converted some $COO^-$ groups back to COOH. To prepare for titration, all $COO^-$ were first converted to COOH with added HCl. In titration, the initial decrease in conductivity in the parabolic-shape titration curves with increasing NaOH concentrations was due to the neutralization of excess HCl (Figure 3a). The conductivity reached a plateau as NaOH was consumed to convert carboxylic acid to its sodium form, then sharply increased from the excess NaOH. The total COOH+$COO^-$ quantity was calculated based on the NaOH amount added in the plateau regions. HCNF5-30 had a total of 1.09 mmol/g COOH+$COO^-$ content, 20% lower than the 1.36 mmol/g for CNF5-30 (Figure 3a). Doubling NaClO concentration significantly raised COOH+$COO^-$ content to 1.77 mmol/g for HCNF10-30. The original surface primary C6 hydroxyls were calculated based on the individual crystalline dimensions of CNF5-30, HCNF5-30 and HCNF10-30 to be 0.26, 0.26, and 0.25 per anhydroglucose (AG), respectively (Table S1, Supporting Information). If the oxidation reaction occurred on the crystalline surface,[3,26] the extent by which the surface primary hydroxyls was converted to COOH/$COO^-$ groups was calculated from the total COOH+$COO^-$ per AG (Figure 3a) divided by surface primary hydroxyl per AG, to be 85, 69, and 115% for CNF5-30, HCNF5-30, and HCNF10-30, respectively. Under the same TEMPO oxidation at 5 mM NaClO, the surface COOH/$COO^-$ on HCNF5-30 was 16% less than that on CNF5-30, showing reduced cellulose C6 OH to COOH/$COO^-$ conversion in holocellulose. As NaClO doubled to 10 mM per gram of holocellulose, the surface COOH/$COO^-$ of HCNF10-30 increased by 62% to 1.77 mmol per gram of nanofibrils, which was slightly higher than that of CNF (1.68 mmol/g cellulose, i.e. nearly 100% surface C6 OH conversion).[13] The additional 15% surface OH/(COOH +COO−) conversion on HCNF10-30 may be due to the carboxylate groups in the hemicelluloses that was readsorbed to the CNF surfaces or the conversion of some HCNF10-30 surface glucan chains to homopolyglucuronic acid by TEMPO-mediated oxidation.[27]

Conductometric titration was also conducted without adding HCl to retain the $COO^-$, that is, without converting to COOH, where the titration curves represent only neutralization of the COOH present (Figure 3b). The COOH contents calculated based on the NaOH amount added in the initial plateau regions were 0.296, 0.652, and 0.137 mmol COOH per gram of nanofibrils for HCNF5-30, HCNF10-30, and CNF5-30, respectively. Of the total COOH+$COO^-$ contents, 73, 63, and 90% are in the $COO^-$ form in HCNF5-30, HCNF10-30, and CNF5-30, respectively. Because the charge of nanofibrils came from the carboxylate $COO^-$, but not COOH, the charges of HCNF5-30, HCNF10-30, and CNF5-30 were calculated to be 0.80, 1.12, and 1.22 mmol per gram of nanofibrils, respectively.

Therefore, the presence of hemicelluloses has clearly affected TEMPO oxidation and the surface COOH/$COO^-$ contents of the resulted HCs and HCNFs. Initially, hemicelluloses bound to the cellulose surface via hydrogen bonding and van der


DOI: 10.1021/am5079489
ACS Appl. Mater. Interfaces 2015, 7, 4192−4201

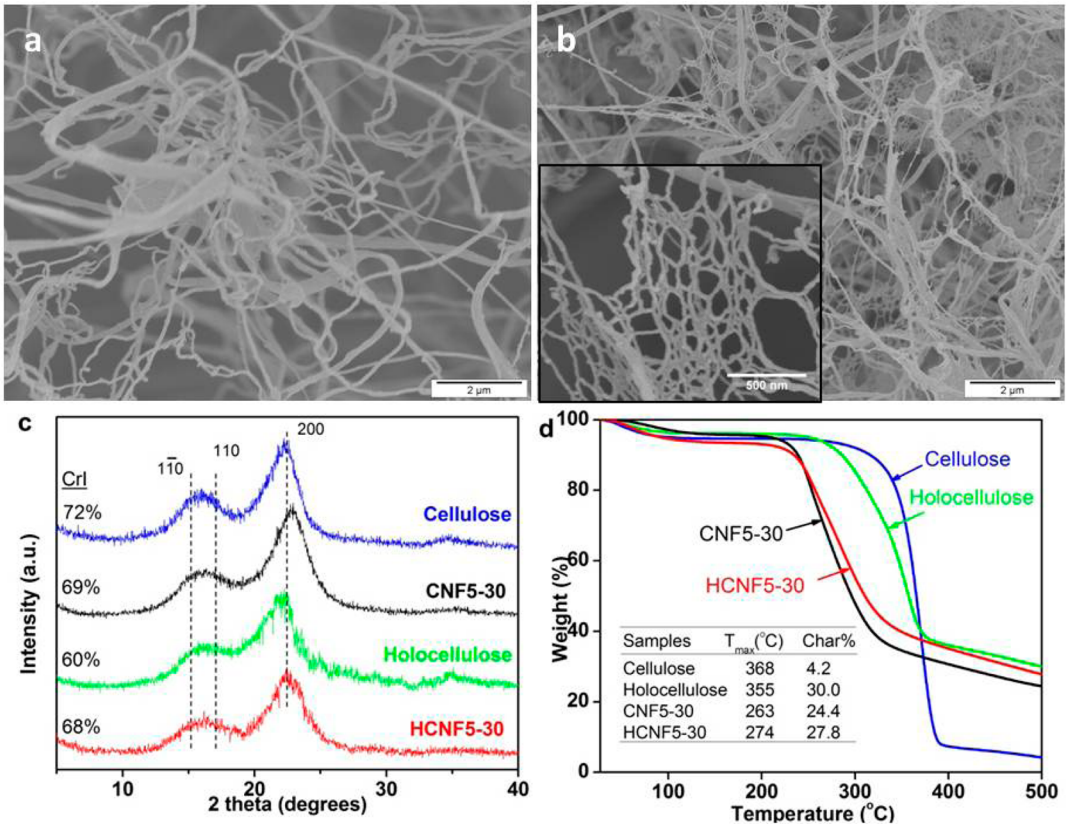


**Figure 4.** Freezing induced self-assembled cellulose structures: SEM images of fibers assembled from HCNF5-30 at (a) 0.1% and (b) 0.01%; (c) X-ray diffractogram; (d) TGA thermograms with maximum degradation temperatures and char residues at 500 °C.

Waals interaction known in higher plants[28−30] may limit the initial access of the oxidation agents. As the oxidation reaction progressed, most hemicelluloses were expected to be converted to soluble sugars such as C2/C3 dicarboxyl xylan,[18,20] consuming the oxidizing agents which otherwise would have reacted with cellulose and resulting in less oxidized cellulose or lower COOH+$COO^-$ content of HCNF5-30 than CNF5-30. When NaClO concentration doubled to 10 mM per gram of holocellulose, more oxidation reagent was available to oxidize cellulose, producing more COOH+$COO^-$ or more oxidized HCNF10-30.

**3.3. Freezing and Freeze-Drying Induced Self-Assembling of HCNFs.** Rapid freezing 0.1% and 0.01% aqueous HCNF5-30 suspensions in liquid nitrogen followed by freeze-drying produced white sponge-like mass of randomly oriented fibers (Figure 4a,b). The nanofibers from 0.1% suspension were averagely 94 ± 33 nm wide and hundreds of micrometers long. These assembled nanofibers were almost 30 times thicker and hundreds of times longer than individual HCNF5-30 (Figure 2), indicating original individual HCNF5-30 nanofibrils associated with each other laterally and, most significantly, longitudinally into larger nanofibers. Few ribbons in 400−1000 nm widths were also observed. From a lower 0.01% concentration, HCNF5-30 also self-assembled into interconnected fibers, except in two populations: much thinner 18 ± 5 nm average diameter nanofibers (Figure 4b) and ultrafine fibers with an average diameter of 164 ± 70 nm.

Intriguingly, the fibers self-assembled from HCNF5-30 are much thinner, only one-fifth of those from CNF5-30 (497 ± 161 nm) from the same 0.1% concentration and under the same condition.[11] Although the lateral dimensions of individual HCNF5-30 and CNF5-30 nanofibrils were similar, the much thinner fibers assembled from HCNF5-30 indicate far lower inter-nanofibril affinity. Because the less oxidized (1.09 vs 1.36 mmol/g total COOH+$COO^-$) and negatively charged (0.80 vs 1.22 mmol per gram of nanofibrils) HCNF5-30 did not assembled to larger fibers, the much reduced assembling was thought to be caused more by the presence of hemicelluloses and possibly silica on the surfaces. Rice straw hemicelluloses contain mainly arabinoxylan which is less hydrophilic than cellulose due to its lack of primary hydroxyls in the xylan backbone. The presence of relatively more hydrophobic xylan, silica, or both made the HCNF5-30 surfaces more heterogeneous, inhibiting nanofibril association in both lateral directions and resulting in less assembled structure. These observations on nanocellulose is consistent with the previous report that hemicellulose decreased the aggregation of the much larger microfibrils by disrupting interfibrillar hydrogen bonding.[14] Besides hemicelluloses and silica, the C6 aldehyde groups in TEMPO-oxidized nanofibrils may also affect the lyophilization-induced self-assembling behaviors of CNFs and HCNFs. However, the aldehyde contents of CNF5-30 and HCNF5-30 were very low, at 0.32 and 0.23 mmol/g, respectively (Supporting Information), compared to the COOH/$COO^-$ content. Because the aldehyde content of the CNF5-30 and HCNF5-30 was comparably low, the differences in their self-assembled structures were attributed mainly to the presence of residual hemicelluloses on their surfaces.

Cellulose, holocellulose, self-assembled CNF5-30, and HCNF5-30 exhibited the same three cellulose I characteristic peaks at $2\theta$ = 14.5, 16.6, and 22.7° assigned to 1$\bar{1}$0, 110, and 200 crystallographic planes, respectively, but different crystal-


DOI: 10.1021/am5079489
ACS Appl. Mater. Interfaces 2015, 7, 4192−4201

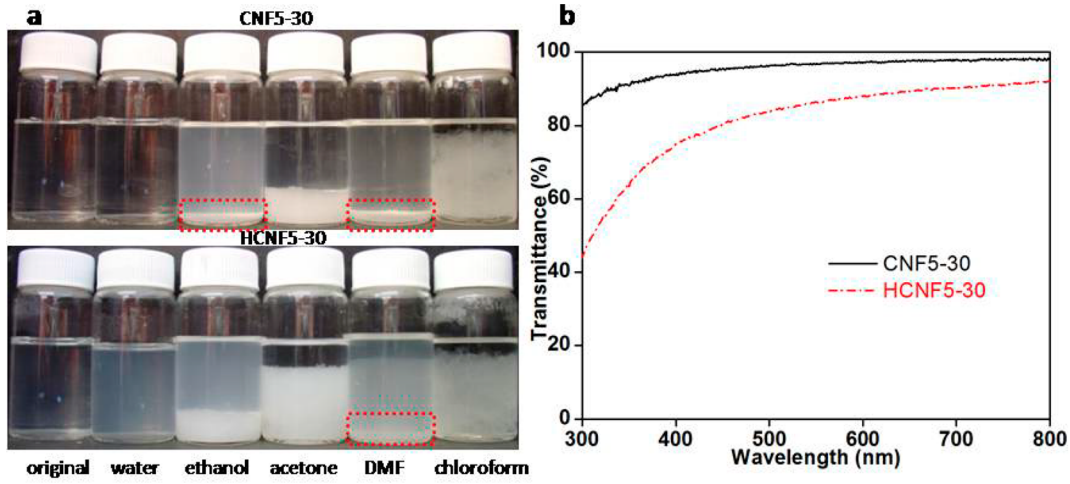


**Figure 5.** (a) Redispersions of self-assembled (top) CNF5-30 and (bottom) HCNF5-30 after 1 day in (left to right) original and redispersed in water, ethanol, acetone, DMF, and chloroform. The red boxes indicate the formation of organogels. (b) Light transmittance of redispersed aqueous suspensions.

linity indexes (CrI) of 72, 60, 69, and 68%, respectively. The lower CrI of holocellulose reflects the interference of amorphous hemicelluloses and silica. The CrI index of CNF5-30 and HCNF5-30 was lower than pure cellulose, consistent with their more defibrillated and oxidized state.[13] The CrI of HCNF5-30 was higher than holocellulose and close to CNF5-30 which was consistent with the fact that most amorphous hemicelluloses in holocellulose were dissolved during TEMPO oxidation.[18,20]

The TGA curves of cellulose, holocellulose, CNF5-30 and HCNF5-30 all showed initial small mass loss of 3−5% from evaporation of adsorbed moisture, followed by the rapid mass loss from cellulose decomposition and final mass loss from charring (Figure 4d). The temperature where maximum weight loss occurs, $T_{max}$, (Figure S2, Supporting Information) was highest for cellulose (368 °C) followed by holocellulose (355 °C) and then the nanofibrils. The first derivative curve of holocellulose showed an additional smaller hemicellulose decomposition peak at around 300 °C (Figure S2, Supporting Information). The $T_{max}$ of HCNF5-30 was 274 °C, higher than CNF5-30 at 263 °C possibly due to presence of more thermal stable silica. The char residue of holocellulose was 6.1 times higher than cellulose, while the char residue of HCNF5-30 was 12% higher than that of CNF5-30, again attributed to the presence of silica. The char residues of CNF5-30 and HCNF5-30 were approximately 5 times higher than that of cellulose, which may be due to increased interfacial interactions of hydrogen bonding among the hydroxyls and carboxyls in the self-assembled structures.[13]

**3.4. Aqueous and Organic Dispersion and Redispersion of Self-Assembled Fibers.** To further discern the impact of residual hemicelluloses, we made observations on the redispersibility of the self-assembled structures in aqueous and organic solvents as well as on solvent exchange of the aqueous suspensions to organic solvents. CNF5-30 and HCNF5-30 self-assembled from 0.1% aqueous suspensions were dispersed in water as well as various organic solvents to the same 0.1% concentration, aided by mechanical stirring (1200 rpm) combined with either low-power ultrasonication (40 kHz, 130 w) or high-power ultrasonication (20 kHz, 600 w). With repeated mechanical stirring and low-power ultrasonication, the redispersed aqueous suspension of self-assembled CNF5-30 was transparent, but that from HCNF5-30 remained relatively turbid. When these suspensions were diluted to 0.0005% followed by sonication and deposited on mica surfaces for AFM observation, both CNF and HCNF appeared as individually separated nanofibrils (Figure S3, Supporting Information), similar to their original morphologies (Figure 2). With high-power ultrasonication alone, the redispersed HCNF5-30 suspension showed increased light transmittance, but still less transparent than the redispersed CNF5-30 (Figure 5). Therefore, the self-assembled CNF and HCNF fibers could be redispersed in water at 0.1% concentration, with HCNFs being less uniform.

The self-assembled CNF5-30 and HCNF5-30 were also redispersed in DMF, ethanol and acetone, aided by either mechanical stirring or ultrasonication. While high-power ultrasonication disrupted the assembled CNF and HCNFs structures, none remained as stable suspension over time (Figure 5a). After settling for 1 day under the ambient condition, most CNF5-30 redispersed in ethanol and DMF precipitated and gelled, but could be broken up by vigorous hand shaking. When allowed to settle for 5 days, all CNF5-30 settled at the bottom leaving the top ethanol and DMF suspensions clear (not shown). The CNF5-30 redispersed in acetone settled to form white fluffy aggregates while that redispersed in chloroform appeared as suspension of particles that were larger than those in other solvents. Redispersed HCNF5-30 also precipitated and gelled in DMF but was less integrated and easier to be broken up by vigorous hand shaking than was the precipitate that formed from CNF5-30. The self-assembled HCNFs redispersed in ethanol and acetone did not gel, but they formed stabilized HCNF-rich phases at the bottom that were larger than CNF in the same solvents. All HCNF5-30 dispersed in DMF and ethanol settled after 5 days, leaving the top suspension clear (not show). Most HCNF5-30 redispersed in chloroform remained suspended as particles in the middle of the vial, similar to CNF5-30.

Aqueous CNF5-30 and HCNF5-30 suspensions were solvent exchanged to organic solvents, all at 0.1% concentration. Both CNF 5-30 and HCNF5-30 solvent exchanged to DMF as clear dispersions and remained stable for over a month, in contrast to gelation observed in DMF redispersions of their self-assembled structures. AFMs of the freshly exchanged suspensions diluted


DOI: 10.1021/am5079489
ACS Appl. Mater. Interfaces 2015, 7, 4192−4201

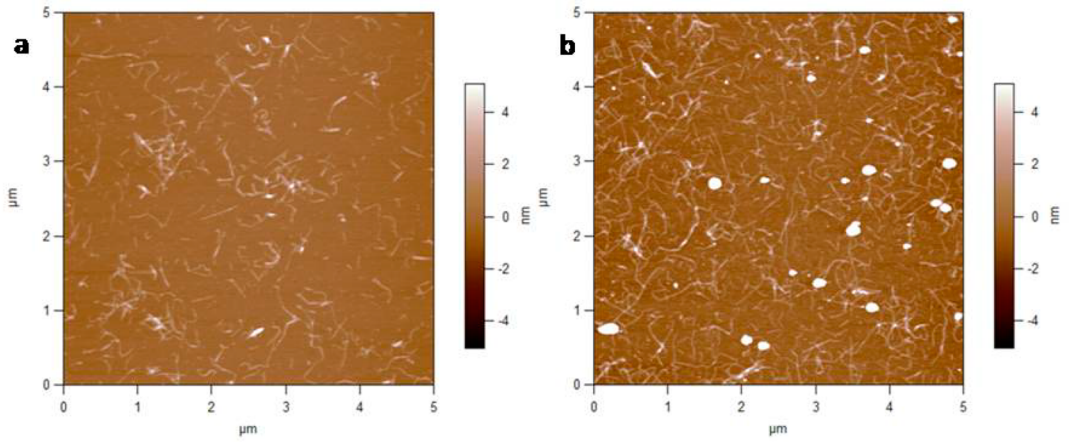


**Figure 6.** AFM images of (a) CNF5-30 and (b) HCNF5-30 prepared from solvent exchanged DMF dispersions.

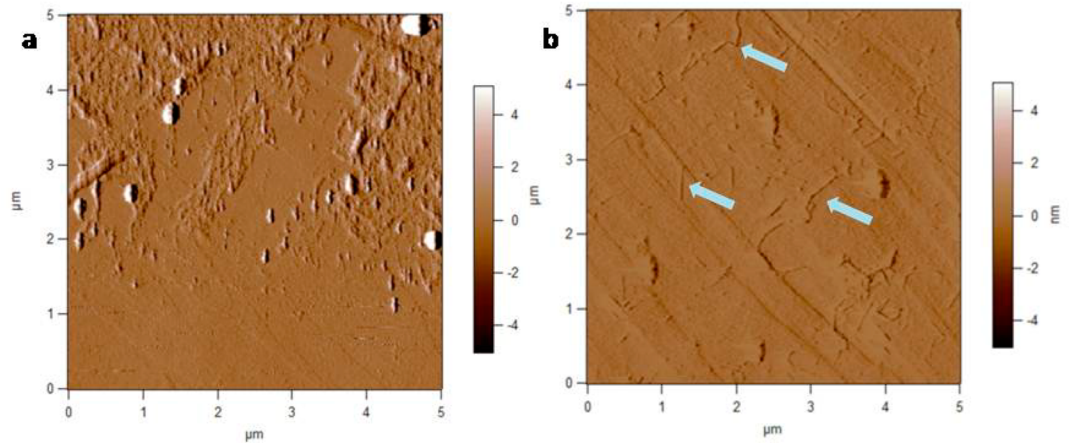


**Figure 7.** AFM phase image showing the dispersion of (a) CNF or (b) HCNF on graphite surface (stripes on the image are the texture of graphite surface used). The arrows on image b indicate the highly dispersed individual HCNF nanofibrils.

to 0.0005% showed individual CNFs or HCNFs with height ranging from 1 to 5 nm (Figure 6), similar to their aqueous original (Figure 2d,e). However, the presence of numerous shorter 100−500 nm long nanofibrils indicated fibril breakage from ultrasonication. Some white spots found in HCNFs were likely silica, as observed before (Figure 2f). CNF and HCNF dispersions exchanged in either acetone or ethanol were translucent but formed gel on the vial wall (Figure S4, Supporting Information). On the basis of the above results, aqueous HCNFs and CNF could be solvent exchanged to clear and stable DMF suspensions, but not to acetone and ethanol. Ultrasonication did cause nanofibril breakage.

The much higher solubility parameter of cellulose, i.e., 55.7 $MPa^{0.5}$ ($\delta d$ = 11.7 $MPa^{0.5}$, $\delta p$ = 35.9 $MPa^{0.5}$, and $\delta h$ = 42.2 $MPa^{0.5}$),[31] than water ($\delta$ = 48.0 $MPa^{0.5}$, $\delta d$ = 15.5 $MPa^{0.5}$, $\delta p$ = 16.0 $MPa^{0.5}$, and $\delta h$ = 42.3 $MPa^{0.5}$) make the highly crystalline nanocellulose to be well dispersed in water as a transparent aqueous suspension. The higher dielectric constant and hydrogen bonding ability of water are capable disrupting the hydrogen bonds among freeze-dried CNFs to redisperse into a transparent aqueous suspension. From a Hansen solubility parameter (HSP) point of view,[32] rice straw hemicelluloses (mostly arabinoxylan) adsorb on cellulose via relatively high-HSP hydroxyl side chains leaving low-HSP side chain such as acetyl (if any) facing outward. Therefore, HCNFs are thought to self-assemble via both hydrophobic and hydrophilic interactions, whereas CNF self-assembled mainly through hydrophilic interactions. The more hydrophobically bound self-assembled HCNFs would be more resistant to be dispersed into individual nanofibrils in water, thus remained as larger aggregates, but would have better affinity to ethanol, acetone, and DMF to form larger nanofibrils-rich phase in these solvents.

When solvent exchange directly, both CNFs and HCNFs could be well dispersed in DMF to stable suspensions, but not in other organic solvents. A previous work attributed the dispersibility of oxidized cellulose nanofibrils in DMF to its higher dielectric constant that facilitates the dissociation of carboxyl groups.[33] While gelation occurred to 0.2% CNF5-30 exchanged for DMF, gelation was observed at above 0.3% for HCNF5-30 (not shown), again affirming the better dispersion of HCNFs in DMF than CNF5-30 facilitated by the relatively more hydrophobic hemicelluloses. Due to close density of chloroform ($d$ = 1.5 $g/cm^3$) to cellulose, both CNFs and HCNFs suspended in the middle of chloroform as largest fiber aggregates.

To further differentiate the hydrophobicity of CNF5-30 and HCNF5-30, we deposited a drop of each of their 0.0001 wt % dilutions and air-dried onto a freshly cleaved highly ordered pyrolytic graphite (HOPG) surface with a reported 70° high water contact angle.[34] After drying, most HCNFs concentrated along the perimeter of the original droplet, forming a ring


DOI: 10.1021/am5079489
ACS Appl. Mater. Interfaces 2015, 7, 4192−4201

(Figure S5, Supporting Information), while few HCNFs remained at the center as individual nanofibrils (Figure 7b, arrows). This observation was similar to the dispersion of HCNFs or CNFs on highly hydrophilic mica (Figure 2d,e). However, aqueous CNF5-30 did not form ring structure when dried on the same HOPG surface, instead aggregated at the center of the original aqueous drop (Figure 7a). In the coffee ring effect,[35] the ring deposit along the perimeter could only be observed when the particles in the suspension have a strong attractive interaction with the solid surface. The above observation clearly shows HCNFs to be more hydrophobic than CNF and attracted to and dispersed better on the relatively hydrophobic HOPG while still retaining sufficient hydrophilicity to be well dispersed on the hydrophilic mica surface. The associate of hemicelluloses to HCNFs changed its surface property and made it more hydrophobic than CNFs.

## CONCLUSIONS

Holocellulose nanofibrils (HCNFs) have been produced from rice straw holocellulose by TEMPO-mediated oxidation (5 mmol/g NaClO/holocellulose) and mechanical blending (30 min) at a 33.7% yield (based on original rice straw mass), higher than 29.1% of cellulose nanofibrils (CNFs) produced from pure cellulose by the same procedures. HCNFs had a similar average width (2.92 ± 1.10 nm) and height (1.36 ± 0.62 nm) as CNFs but appeared longer, containing mostly micrometer-long nanofibrils. While the TEMPO-mediated oxidation removed majority of hemicelluloses and some silica, HCNFs contained a small amount of silica and hemicelluloses. The surface OH to $COOH+COO^-$ conversion on HCNFs (69%) was lower than CNFs (85%), generating 1.09 mmol/g total $COOH+COO^-$ content, 25% lower than the 1.36 mmol/g for CNFs and the lower proportion of the ionized carboxylate $COO^-$ (75 vs 90%). Doubling either NaClO concentration or mechanical defibrillation time increased the surface $COOH+COO^-$ to 1.77 mmol/g but decreased the yield. Self-assembling of HCNFs induced by rapid freezing and freeze-drying was substantially reduced by presence of hemicelluloses and silica to much thinner nanofibers, one-fifth or less in average widths, under the same conditions while possessing the same crystal structure and thermal properties. Both self-assembled CNF and HCNF could be redispersed in water, but gelled in DMF and formed various suspended aggregated, particulated, or nanofibrils-rich phase in ethanol, acetone, and chloroform. Both aqueous CNF and HCNF suspensions could also be solvent exchanged with DMF—HCNF DMF suspension is more stable—but not other organic solvents. HCNFs also showed affinity to both hydrophilic and hydrophobic surfaces as opposed to CNF's affinity to hydrophilic surface. In comparison, the amphiphilic rice straw HCNFs exhibited more hydrophobic characteristics and self-assembled less to form much finer fibers. By streamlining the isolating process without alkaline dissolution of hemicelluloses, rice straw HCNFs possessed unique properties while remaining similar to CNFs in high crystallinity and thermal properties for more expanded applications.

## ASSOCIATED CONTENT

### Supporting Information

Aldehyde content measurement method; X-ray diffraction method; IR spectrum of precipitate centrifuged from defibrillated HCF5; first derivative of thermogravimetric curves of rice straw cellulose, holocellulose, CNF, and HCNF; AFM images of freeze-dried CNF and HCNF dispersion in water; optical image of CNF and HCNF dispersion in ethanol and acetone; optical image of HCNF deposit on HOPG surface; and crystallite dimensions and calculated surface C6 primary hydroxyls for CNF and HCNF. This material is available free of charge via the Internet at http://pubs.acs.org.

## AUTHOR INFORMATION

### Corresponding Author

*Tel: +1 530 752 0843; ylhsieh@ucdavis.edu.

### Notes

The authors declare no competing financial interest.

## ACKNOWLEDGMENTS

Financial support for this research from USDA NIFA (2011-67021-20034) and California Rice Research Board (RU-9) is greatly appreciated. The authors are grateful to Dr. Jiang Feng for assistance with SEM and aldehyde content measurements.

## REFERENCES

(1) Moon, R. J.; Martini, A.; Nairn, J.; Simonsen, J.; Youngblood, J. Cellulose Nanomaterials Review: Structure, Properties and Nanocomposites. *Chem. Soc. Rev.* **2011**, *40*, 3941−3994.

(2) Nakagaito, A. N.; Yano, H. Novel High-Strength Biocomposites Based on Microfibrillated Cellulose Having Nano-Order-Unit Web-Like Network Structure. *Appl. Phys. A: Mater. Sci. Process.* **2005**, *80*, 155−159.

(3) Isogai, A.; Saito, T.; Fukuzumi, H. Tempo-Oxidized Cellulose Nanofibers. *Nanoscale* **2011**, *3*, 71−85.

(4) Henriksson, M.; Henriksson, G.; Berglund, L. A.; Lindstrom, T. An Environmentally Friendly Method for Enzyme-Assisted Preparation of Microfibrillated Cellulose (MFC) Nanofibers. *Eur. Polym. J.* **2007**, *43*, 3434−3441.

(5) Paakko, M.; Ankerfors, M.; Kosonen, H.; Nykanen, A.; Ahola, S.; Osterberg, M.; Ruokolainen, J.; Laine, J.; Larsson, P. T.; Ikkala, O.; Lindstrom, T. Enzymatic Hydrolysis Combined with Mechanical Shearing and High-Pressure Homogenization for Nanoscale Cellulose Fibrils and Strong Gels. *Biomacromolecules* **2007**, *8*, 1934−41.

(6) Saito, T.; Isogai, A. Tempo-Mediated Oxidation of Native Cellulose. The Effect of Oxidation Conditions on Chemical and Crystal Structures of the Water-Insoluble Fractions. *Biomacromolecules* **2004**, *5*, 1983−1989.

(7) Saito, T.; Hirota, M.; Tamura, N.; Kimura, S.; Fukuzumi, H.; Heux, L.; Isogai, A. Individualization of Nano-Sized Plant Cellulose Fibrils by Direct Surface Carboxylation Using Tempo Catalyst under Neutral Conditions. *Biomacromolecules* **2009**, *10*, 1992−6.

(8) Binod, P.; Sindhu, R.; Singhania, R. R.; Vikram, S.; Devi, L.; Nagalakshmi, S.; Kurien, N.; Sukumaran, R. K.; Pandey, A. Bioethanol Production from Rice Straw: An Overview. *Bioresour. Technol.* **2010**, *101*, 4767−4774.

(9) Lu, P.; Hsieh, Y. L. Preparation and Characterization of Cellulose Nanocrystals from Rice Straw. *Carbohydr. Polym.* **2012**, *87*, 564−573.

(10) Hessien, M. M.; Rashad, M. M.; Zaky, R. R.; Abdel-Aal, E. A.; El-Barawy, K. A. Controlling the Synthesis Conditions for Silica Nanosphere from Semi-Burned Rice Straw. *Mater. Sci. Eng., B* **2009**, *162*, 14−21.

(11) Jiang, F.; Hsieh, Y. L. Chemically and Mechanically Isolated Nanocellulose and Their Self-Assembled Structures. *Carbohydr. Polym.* **2013**, *95*, 32−40.

(12) Lu, P.; Hsieh, Y. L. Preparation and Properties of Cellulose Nanocrystals: Rods, Spheres, and Network. *Carbohydr. Polym.* **2010**, *82*, 329−336.

(13) Jiang, F.; Han, S.; Hsieh, Y.-L. Controlled Defibrillation of Rice Straw Cellulose and Self-Assembly of Cellulose Nanofibrils into Highly Crystalline Fibrous Materials. *RSC Adv.* **2013**, *3*, 12366−12375.

(14) Chaker, A.; Alila, S.; Mutjé, P.; Vilar, M.; Boufi, S. Key Role of the Hemicellulose Content and the Cell Morphology on the



DOI: 10.1021/am5079489
*ACS Appl. Mater. Interfaces* 2015, 7, 4192−4201

Nanofibrillation Effectiveness of Cellulose Pulps. *Cellulose* **2013**, *20*, 2863−2875.
(15) Duchesne, I.; Hult, E.; Molin, U.; Daniel, G.; Iversen, T.; Lennholm, H. The Influence of Hemicellulose on Fibril Aggregation of Kraft Pulp Fibres as Revealed by FE-SEM and CP/MAS $^{13}$C-NMR. *Cellulose* **2001**, *8*, 103−111.
(16) Oksanen, T.; Buchert, J.; Viikari, L. The Role of Hemicelluloses in the Hornification of Bleached Kraft Pulps. *Holzforschung* **1997**, *51*, 355−360.
(17) Hannuksela, T.; Holmbom, B. Sorption of Mannans to Different Fiber Surfaces: An Evolution of Understanding. In *Hemicelluloses: Science and Technology*; American Chemical Society: 2003; Chapter 15, pp 222−235.
(18) Okita, Y.; Saito, T.; Isogai, A. Tempo-Mediated Oxidation of Softwood Thermomechanical Pulp. *Holzforschung* **2009**, *63*, 529−535.
(19) Puangsin, B.; Fujisawa, S.; Kuramae, R.; Saito, T.; Isogai, A. Tempo-Mediated Oxidation of Hemp Bast Holocellulose to Prepare Cellulose Nanofibrils Dispersed in Water. *J. Polym. Environ.* **2013**, *21*, 555−563.
(20) Kuramae, R.; Saito, T.; Isogai, A. Tempo-Oxidized Cellulose Nanofibrils Prepared from Various Plant Holocelluloses. *React. Funct. Polym.* **2014**, *85*, 126−133.
(21) Reddy, N.; Yang, Y. Biofibers from Agricultural Byproducts for Industrial Applications. *Trends Biotechnol.* **2005**, *23*, 22−27.
(22) Van Soest, P. J. Rice Straw, the Role of Silica and Treatments to Improve Quality. *Anim. Feed Sci. Technol.* **2006**, *130*, 137−171.
(23) Agbagla-Dohnani, A.; Noziere, P.; Gaillard-Martinie, B.; Puard, M.; Doreau, M. Effect of Silica Content on Rice Straw Ruminal Degradation. *J. Agric. Sci.* **2003**, *140*, 183−192.
(24) Johnson, R.; Zink-Sharp, A.; Renneckar, S.; Glasser, W. A New Bio-Based Nanocomposite: Fibrillated Tempo-Oxidized Celluloses in Hydroxypropylcellulose Matrix. *Cellulose* **2009**, *16*, 227−238.
(25) Li, Q.; Renneckar, S. Molecularly Thin Nanoparticles from Cellulose: Isolation of Sub-Microfibrillar Structures. *Cellulose* **2009**, *16*, 1025−1032.
(26) Meng, Q.; Li, H.; Fu, S.; Lucia, L. A. The Non-Trivial Role of Native Xylans on the Preparation of Tempo-Oxidized Cellulose Nanofibrils. *React. Funct. Polym.* **2014**, *85*, 142−150.
(27) Hirota, M.; Furihata, K.; Saito, T.; Kawada, T.; Isogai, A. Glucose/Glucuronic Acid Alternating Co-Polysaccharides Prepared from Tempo-Oxidized Native Celluloses by Surface Peeling. *Angew. Chem., Int. Ed.* **2010**, *49*, 7670−7672.
(28) Mazeau, K.; Charlier, L. The Molecular Basis of the Adsorption of Xylans on Cellulose Surface. *Cellulose* **2012**, *19*, 337−349.
(29) Hanus, J.; Mazeau, K. The Xyloglucan-Cellulose Assembly at the Atomic Scale. *Biopolymers* **2006**, *82*, 59−73.
(30) Pauly, M.; Albersheim, P.; Darvill, A.; York, W. S. Molecular Domains of the Cellulose/Xyloglucan Network in the Cell Walls of Higher Plants. *Plant J.* **1999**, *20*, 629−39.
(31) Bochek, A. M. Effect of Hydrogen Bonding on Cellulose Solubility in Aqueous and Nonaqueous Solvents. *Russ J. Appl. Chem.* **2003**, *76*, 1711−1719.
(32) Hansen, C. M.; Bjorkman, A. The Ultrastructure of Wood from a Solubility Parameter Point of View. *Holzforschung* **1998**, *52*, 335−344.
(33) Okita, Y.; Fujisawa, S.; Saito, T.; Isogai, A. Tempo-Oxidized Cellulose Nanofibrils Dispersed in Organic Solvents. *Biomacromolecules* **2011**, *12*, 518−522.
(34) Yang, H.; Fung, S. Y.; Pritzker, M.; Chen, P., Modification of Hydrophilic and Hydrophobic Surfaces Using an Ionic-Complementary Peptide. *PLoS One* **2007**, *2*.
(35) Deegan, R. D.; Bakajin, O.; Dupont, T. F.; Huber, G.; Nagel, S. R.; Witten, T. A. Capillary Flow as the Cause of Ring Stains from Dried Liquid Drops. *Nature* **1997**, *389*, 827−829.


DOI: 10.1021/am5079489
*ACS Appl. Mater. Interfaces* 2015, 7, 4192−4201